A Novel Concept of a Single-Phase Cascaded H-Bridge Multilevel Inverter for Grid-Connected Photovoltaic Systems

Vu Hoang Phuong, Nguyen Khac Hieu*, Pham Viet Phuong, Tran Manh Hung

Hanoi University of Science and Technology - No. 1, Dai Co Viet Str., Hai Ba Trung, Ha Noi, Viet Nam

Received: April 02, 2018; Accepted: November 26, 2018

Abstract

A single-phase cascaded H-bridge multilevel inverter has several DC links that allows the system to have the capability of independently voltage control to track the maximum power point in each string connected to each H-bridge. This characteristic can increase the efficiency of the PV system in case of mismatch in the strings, due to unequal solar radiation and temperature. This paper presents a generalized design method for controllers of a multi-loop control scheme applying for grid-connected photovoltaic systems using a single-phase cascaded H-bridge multilevel inverter. The simulation results were carried out by Matlab/Simpower Systems to validate the proposed method under different operating conditions of PV.

Keywords: Cascaded H-bridge multilevel inverter, Grid-connected photovoltaic systems, A multi-loop control scheme

1. Introduction

Nowadays, grid-connected single-phase photovoltaic systems are recognized for their contribution to clean power generation. A primary goal of these systems is to increase the energy injected to the grid by keeping track of the maximum power point of the panel. Because of the mismatch in solar irradiance, the different temperature, aging of the PV modules or the accumulation of dust on the surface of the modules, the generation efficiency of the PV system can be decreased. To avoid this problem, the multi-string topology in which consists of several PV strings that connect DC/DC converters to a general DC/AC inverter was proposed [?]. However, the disadvantages of this two stages power conversion topology is low efficiency. In these days, the cascaded H-bridge (CHB) topology is widely used for PV applications [1]. A multi-level inverter can generate low harmonic voltage waveforms with low frequency to obtain higher efficiency. Additionally, the multilevel topology has several DC links which makes it possibly to control the voltage independently. As a result, individual maximum power point tracking (MPPT) control in each string can be achieved, and the energy harvested from PV panels can be maximized.

In single-phase cascaded H-bridge multilevel inverter for grid-connected photovoltaic systems, the well-known control block has been suggested by many researchers [2]-[6] in which consits of a PI used at the AC side to track a current reference in order to eliminate the steady-state error. The control signals are generated to each switching device of each H-bridge by phase shifted carrier PWM method. However, the determination process to get parameters of PR current controller is very difficult in practise, especially when CHB is connected to grid through a LCL filter [7],[8]. In some studies, many trial and error procedures have been carried out to obtain a set of parameters of PR regulators [9]. Another approach to design PR controllers is based on the SISO design tool in MATLAB and system dynamic response [10], which is time-consuming and not generalized.

The authors of this paper propose a systematic and generalized design method for PR current controller in LCL-type grid-connected cascaded H-bridge multilevel inverter to guarantee system stability. After all, the designed PR current controller is built-in the control block and MPPT algorithm of a 7-level cascaded multilevel inverter to maximize the gererated energy, when PV modules work in conditions with different irradiance and temperature. Simulation results was carried out by Matlab/Simpower Systems to demonstrate the proposed control scheme.

2. Control scheme

2.1. The single-phase cascaded H-bridge multilevel inverter

The CHB multilevel inverter topology consists of three H-bridge converters connected in series to generate a seven-level voltage waveform. As a result, the synthesized current harmonics is reduced, and the

* Corresponding author: Tel.: (+84)904691182
Email: hieu.nguyenkhac@hust.edu.vn

number of the output filters can also be reduced. As shown in Fig.1, the CHB multilevel inverter is connected to the grid through a LCL filter, which is used to reduce the switching harmonics in the current.

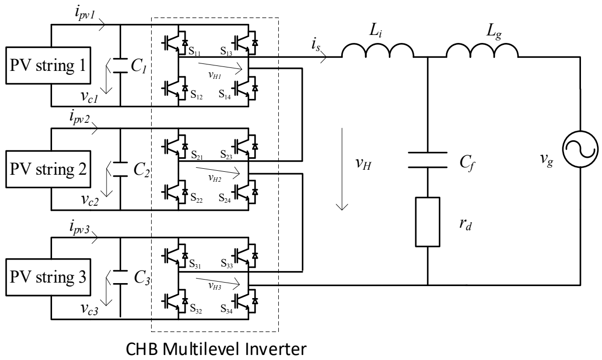

Fig. 1. Seven-level cascaded multilevel inverter.

2.2. Proposed control scheme

The control strategy is based on the classical scheme for the control of a single H-bridge converter connected to the grid and integrated MPPT algorithm to obtain the maximum power from each PV array [2]-[6]. This paper proposed a control scheme, which includes three control loops as shown in Fig.2. The PI controllers regulate the capacitor voltage in each DC link and total DC-link voltage to reference voltages, the values are calculated from MPPT algorithm. In order to protect IGBTs of inverter and get sinusoidal current, a PR controller is used. In addition, the lowpass-filter with 100Hz cross –over frequency is use for measurement of the DC voltages to mitigate the harmonic components in the current [2]. The phase-shifted PWM switching scheme is applied to control the IGBT of each full-bridge.

2.2.1. Current Loop

The transfer function for the inverter-side current i_s to inverter-side voltage with the damping resistor are given as follows:

$$G_{vi_s}(s)=\left.\frac{i_s(s)}{v_s(s)}\right|_{e_n=0}=\frac{1}{Ls}\frac{\left(s^2+r_dC_fz_{LC}^2s+z_{LC}^2\right)}{\left(s^2+r_dC_f\omega_{res}^2s+\omega_{res}^2\right)} \quad (1)$$

where $z_{LC}^2=\left[L_gC_f\right]^{-1}$, $\omega_{res}^2=\left(L_g+L_i\right)z_{LC}^2/L_i$, and ω_{res} is the resonance frequency of the LCL filter [14].

The PR controller can be successfully applied to single phase grid-connected [11], the transfer function of an non-ideal PR controller is given in (2) .

$$G_{PR}(s)=k_p+\frac{2k_r\omega_{PRc}s}{s^2+2\omega_{PRc}s+\omega_h^2} \quad (2)$$

With ω_{PRc} being the bandwidth at -3dB cutoff frequency of the controller to reduce the sensitivity toward frequency variation in grid power, the gain of the controller at $\left(\omega_h\pm\omega_{PRc}\right)$ is approximated to $k_r/\sqrt{2}$. In [11], the frequency response characteristics of the non-ideal PR controller at the selected resonant frequency are calculated as shown in equations (3) and (4).

$$\left|G_{PR}(j\omega)\right|=\frac{\sqrt{k_p^2\left(\omega_h^2-\omega^2\right)^4+\left(\omega_h^2-\omega^2\right)^2\left(\omega_{PRc}\omega\right)^2\left(8k_p^2+8k_pk_r+4k_r^2\right)+16\left(\omega_{PRc}\omega\right)^4\left(k_p+k_r\right)^2}}{\left(\omega_h^2-\omega^2\right)^2+4\left(\omega_{PRc}\omega\right)^2} \quad (3)$$

$$\angle G_{PR}(j\omega)=\arctan\frac{2\omega_{PRc}\omega}{\omega_h^2-\omega^2}\left(1+\frac{k_r}{k_p}\right)-\arctan\frac{2\omega_{PRc}\omega}{\omega_h^2-\omega^2} \quad (4)$$

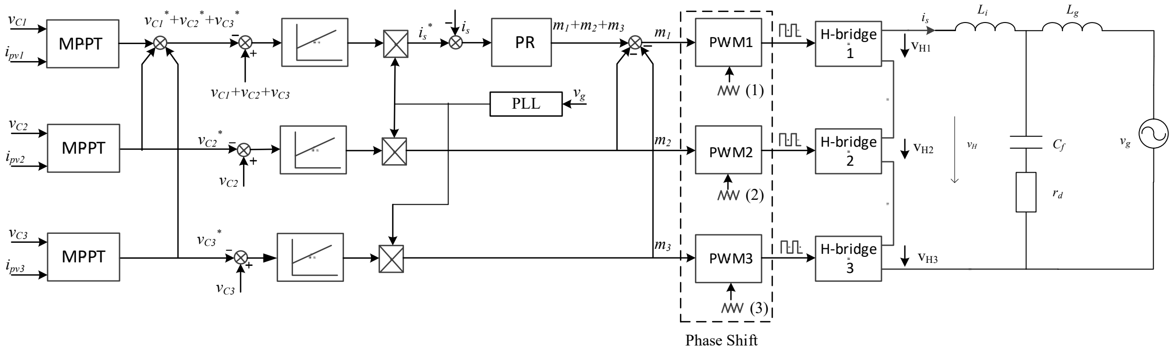

Fig. 2. The control scheme of Seven-level cascaded multilevel inverter.

At the cross-over frequency, the magnitude-frequency response of the system is unity, from (3) the controller gain k_p of PR controllers is approximated as follows:

$$\left(\left|G_{PR}(j\omega)\right|_{\omega=\omega_C}\right)\left|G_{vi}(j\omega)\right|_{\omega=\omega_C}=1$$
$$\rightarrow k_p \approx \frac{1}{\left|G_{vi}(j\omega)\right|_{\omega=\omega_C}} \quad (5)$$

The PM of the PR controller is determined based on the desired value PM of the system's open-loop transfer function the cross-over frequency ω_c, which is given in equation (6).

$$PM = \angle G_{PR}(j\omega)\big|_{\omega=\omega_C} + \angle G_{vi}(j\omega)\big|_{\omega=\omega_C} + 180^0 \quad (6)$$

Since the PM of system is limited by its minimum and maximum values, the PM of the PR controller is thus calculated as follows:

$$A_1 \le \angle G_{PR}(j\omega)\big|_{\omega=\omega_C} \le A_2 \quad (7)$$

Where:

$$A_1 = \min(PM) - \left[\angle G_{vi}(j\omega)\big|_{\omega=\omega_C} + 180^0\right]$$
$$A_2 = \max(PM) - \left[\angle G_{vi}(j\omega)\big|_{\omega=\omega_C} + 180^0\right]$$

Substituting (4) into (7), the maximum and minimum of k_r is determined as shown in equation (8)

$$A_1 \le \arctan\frac{2\omega_{PRc}\omega}{\omega_h^2-\omega^2}\left(1+\frac{k_r}{k_p}\right) - \arctan\frac{2\omega_{PRc}\omega}{\omega_h^2-\omega^2} \le A_2$$
$$\rightarrow k_p\left\{\frac{\omega_h^2-\omega_c^2}{2\omega_{PRc}\omega_c}\tan\left[A_1+\arctan\left(\frac{2\omega_{PRc}\omega_c}{\omega_h^2-\omega_c^2}\right)\right]-1\right\} \le k_r \le k_p\left\{\frac{\omega_h^2-\omega_c^2}{2\omega_{PRc}\omega_c}\tan\left[A_2+\arctan\left(\frac{2\omega_{PRc}\omega_c}{\omega_h^2-\omega_c^2}\right)\right]-1\right\} \quad (8)$$
$$\rightarrow k_p\left\{\frac{1}{M}\tan\left[A_1+\arctan(M)\right]-1\right\} \le k_r \le k_p\left\{\frac{1}{M}\tan\left[A_2+\arctan(M)\right]-1\right\}$$
$$\rightarrow \min(k_r) \le k_r \le \max(k_r)$$

Where $M = \frac{2\omega_{PRc}\omega_c}{\omega_h^2-\omega_c^2}$ and the fundamental frequency of the grid voltage is assumed to vary in the range of ±1Hz, i.e. $\omega_{PRc} = 2\pi$ (rad/s). In [11], the relation between the cross-over frequency f_c, the sampling frequency f_s, and the resonant frequency of LCL filter f_{res} is shown in (9). For multilevel inverter [7], the sampling frequency f_s is determined by switching frequency of each H-bridge $f_{s,H-bridge}$ and level voltage n_{level} in (9).

$$\begin{cases} f_c \le \dfrac{f_s}{10} \\ \dfrac{f_s}{4} \le f_{res} \le \dfrac{f_s}{2} \end{cases}, \; f_s = f_{s,H-bridge}\left(n_{level}-1\right) \quad (9)$$

2.2.2. Voltage Loops

From Fig.1, dynamic of total DC-link voltage and each DC-link voltage can be described by equations (10) and (11).

$$C_1\frac{dv_{c1}}{dt}+C_2\frac{dv_{c2}}{dt}+C_3\frac{dv_{c3}}{dt} = i_{pv1}+i_{pv2}+i_{pv3} - \left(m_1 i_s + m_2 i_s + m_3 i_s\right) \quad (10)$$

$$C_k\frac{dv_{ck}}{dt} = i_{pv\_k} - m_k i_s \quad (11)$$

Where, $m_k\left(k=1\cdots3\right)\in\left[-1,1\right]$ is the modulation index for each H-bridge. To design the controller, equations (10) and (11) are linearized around the nominal operating point. In this paper, it will be considered that the system operates at a nominal radiation of 1000W/m^2 and at 25^{0}C, PV modules are working in the same condition, the grid voltage is 220Vrms at 50Hz, the only DC component of the term $\left(m_1 i_s + m_2 i_s + m_3 i_s\right)$ is considered. The current of the PV panels will be considered as disturbances and cancelled by integrator component of PI [2], [12].

$$\frac{\tilde{v}_{C1}(s)+\tilde{v}_{C2}(s)+\tilde{v}_{C3}(s)}{\tilde{i}_s(s)} = -\frac{\left(m_{1e}+m_{2e}+m_{3e}\right)}{2Cs} \quad (12)$$

$$\frac{\tilde{v}_{C_k}(s)}{\tilde{m}_k(s)} = -\frac{i_{se}}{2C_k s} \quad (13)$$

In order to get dynamic system as 2nd order tranfer function in (14). So that, the parameters of the voltage PI controllers can be calculated by equation (15).

$$W_{2nd}(s)=\frac{2\xi\omega_n s+\omega_n^2}{s^2+2\xi\omega_n s+\omega_n^2} \tag{14}$$

$$\begin{cases} k_{pv}=\dfrac{2\xi\omega_n Cv_{mpp}}{v_{ge}} \\ k_{iv}=\dfrac{\omega_n^2 Cv_{mpp}}{v_{ge}} \end{cases},\begin{cases} k_{pv\_k}=\dfrac{2\xi\omega_n C_k}{i_{se}} \\ k_{iv\_k}=\dfrac{\omega_n^2 C_k}{i_{se}} \end{cases} \tag{15}$$

Where ω_n is natural frequency and ξ is damping coefficient of 2nd Order Systems. In steady state, equilibrium values of inverter current and modulation can be obtained as (16), (17), and the losses in the passive devices and inveter are neglected.

$$P_{out}=\frac{1}{2}v_{ge}i_{se},\quad P_{in}=i_{pv1}v_{c1}+i_{pv2}v_{c2}+i_{pv3}v_{c3}$$
$$\rightarrow i_{se}=\frac{6i_{mpp}v_{mpp}}{v_{ge}} \tag{16}$$

$$(v_{H1e}+v_{H2e}+v_{H3e})^2=v_{ge}^2+(\omega_1 Li_{se})^2$$
$$\rightarrow(m_{1e}+m_{2e}+m_{3e})=\frac{1}{v_{mpp}}\sqrt{v_{ge}^2+(\omega Li_{se})^2} \tag{17}$$

3. Results and analysis `

In this section, simulation results are shown in order to test the proposed control of a single – phase multilevel inverter in grid-tied PV systems. The PV array consists of series 8 panels type of KC200GT that relates to each H-bridge. In the simulation model, in order to obtain the maximum power from each PV string, the incremental conductance (INC) algorithm is used [13] and to achieve the synchronization in single–phase system with high quality, we used a phase-locked loop (PLL) algorithm based on a second-order generalized integrator phase-locked loop (SOGI PLL) [14].

Table 1. Model simulation paramters

Grid Voltage (Vrms)	220V
Fundamental Frequency	50Hz
Inductor/Resistor	10mH/0.01Ω
Capacitor	2200uF
Switching Frequency	1000Hz
PV Panel	KC200GT

The simulation is carried out with two steps. In first step, three PV arrays are operated under the same condition: temperature T = 25°C and irradiance S = 1000 W/m^2. At t=2s, the temperature on the first PV array increases to 40°C, the solar irradiance on the second PV array decreases to 600 W/m^2, the third PV array stays the same irradiance and temperature as the first step.

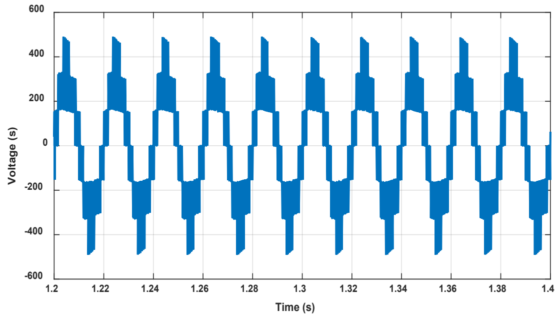

Fig. 3. Inverter voltage output

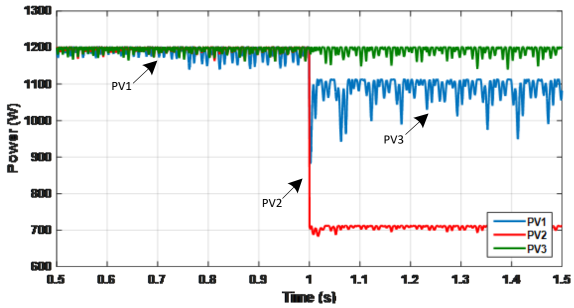

Fig. 4. Power of PV arrays

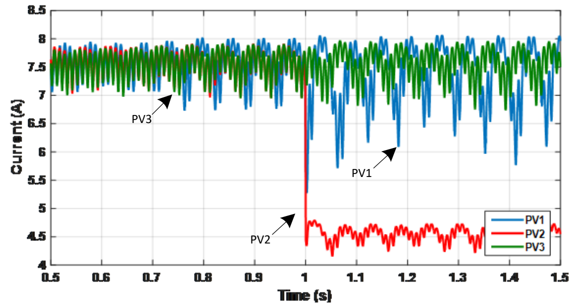

Fig. 5. PV current ouputs

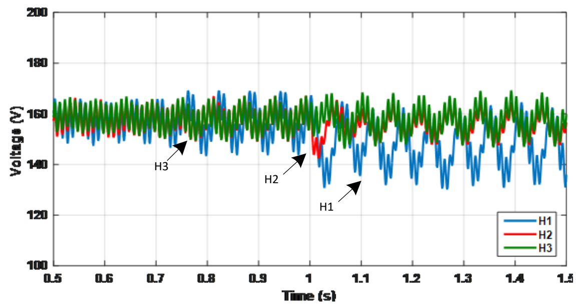

Fig. 6. Voltage on the capacitors

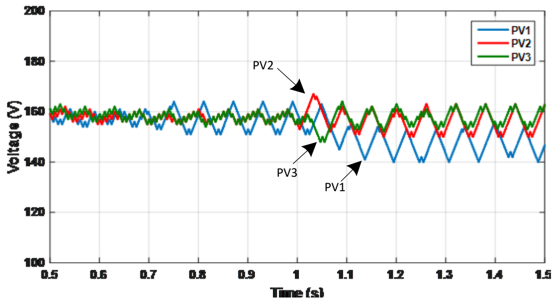

Fig. 7. Voltage reference after tracking on each H-bridge

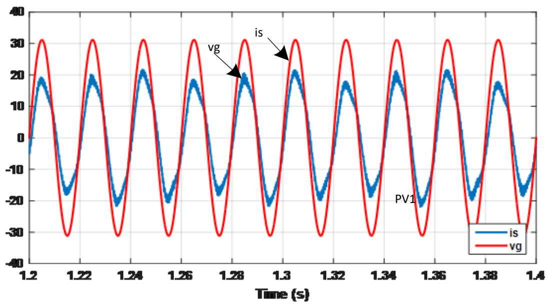

Fig. 8. Output current (10A/div) and grid voltage waveforms (100V/div)

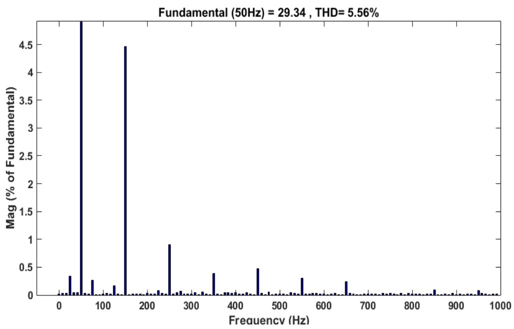

Fig. 9. THD of the grid current

Fig.3 shows inverter output. The inverter output is 7 level waveforms. It helps to reduce the output filters.

Fig.4 shows the power of PV after tracking under different operating points of PV panel. At the beginning, all panel arrays are operated under irradience S = 1000W/m^2 and temperature $T = 25^oC$ and generating maximum power 1200W by 6 panels each array. After $t = 1s$, when temperature over the first array increases to 40 ^{o}C, the solar irradiance over the second array decreases to 600 W/m^2, the power extracted from array 1 is 1112W, from array 2 is 712W, from array 3 is still 1600W.

Fig.5 shows the PV current outputs and Fig.6 shows the DC-link voltage of three H-bridge modules. As the irradiance and the temperature change, the first and second DC-link voltage decrease and track the new MPP voltage as shown in Fig.7

Fig.8 shows the experimental waveforms of grid voltage and output current. Fig.9 shows the THD of output current, it is about 5%, which is satisfy to power quality standards, like IEEE1547 in the US and IEC61727 in Europe. The experimental results aslo show that the grid current has the same phase as the grid voltage and has unity power factor.

4. Conclusion

In this paper, a power conditioning system (PCS) which consists of 7-level cascaded H-bridge multilevel topology for grid-tied low voltage PV systems has been presented. The MPPT algorithm is realized to maximize the energy from PV panels and the control schemes for the cascaced H-bridge multilevel inverter is proposed to improve the efficiency of the system. The simulation results have confirmed the proposed ideas.

Acknowledgments

This research is funded by the Hanoi University of Science and Technology (HUST) under project number T2017-PC-120.

References

[1] Lee, Jong-Pil & Min, Bd & Yoo, Dong-Wook. (2013). Implementation of a High Efficiency Grid-Tied Multi-Level Photovoltaic Power Conditioning System Using Phase Shifted H-Bridge Modules. Journal of Power Electronics. 13. 10.6113/JPE.2013.13.2.296.

[2] E. Villanueva, P. Correa, J. Rodriguez and M. Pacas, Control of a Single-Phase Cascaded H-Bridge Multilevel Inverter for Grid-Connected Photovoltaic Systems, in IEEE Transactions on Industrial Electronics, vol. 56, no. 11, pp. 4399-4406, Nov. 2009.

[3] Bailu Xiao, Ke Shen, Jun Mei, Faete Filho, Leon M. Tolbert, Control of Cascaded H-Bridge Multilevel Inverter with Individual MPPT for Grid-Connected Photovoltaic Generators, 2012 IEEE Energy Conversion Congress and Exposition (ECCE), 15-20 Sept. 2012, pp. 3715 – 3721.

[4] Chao Ma, Jing Wu, Ning Li*, Shaoyuan Li, Control of Single-Phase CHB Grid-Connected Photovoltaic System Under Non-Uniform Irradiation Conditions, 3rd IFAC International Conference on Intelligent Control and Automation Science.September 2-4, 2013. Chengdu, China

[5] C. Boonmee and Y. Kumsuwan, Control of single-phase cascaded H-bridge multilevel inverter with modified MPPT for grid-connected photovoltaic systems, IECON 2013 - 39th Annual Conference of the IEEE Industrial Electronics Society, Vienna, 2013, pp. 566-571.

[6] Sandeep. N, Udaykumar R.Y, Single-Phase Seven-Level Grid-Connected Photovoltaic System with Ripple Correlation Control Maximum Power Point Tracking, INTERNATIONAL JOURNAL of RENEWABLE ENERGY RESEARCH, Vol.6, No.4, 2016.

[7] T. Lahlou, M. Abdelrahem, S. Valdes and H. G. Herzog, Filter design for grid-connected multilevel CHB inverter for battery energy storage systems, 2016 International Symposium on Power Electronics, Electrical Drives, Automation and Motion (SPEEDAM), Anacapri, 2016, pp. 831-836.

[8] Farhadi Kangarlu, M., Babaei, E., Blaabjerg, F. An LCL-filtered Single-phase Multilevel Inverter for Grid Integration of PV Systems. Journal of Operation and Automation in Power Engineering, 2016; 4(1): 54-65.

[9] Chen, K.C. & Salimin, S & Zulkifli, S.A. & Aziz, R. (2017). Single phase inverter system using proportional resonant current control. International Journal of Power Electronics and Drive Systems. 8. 1913-1918. 10.11591/ijpeds. v8i4.pp1913-1918.

[10] Daniel Zammit, Cyril Spiteri Staines, Maurice Apap, John Licari, Design of PR current control with selective harmonic compensators using Matlab, Journal of Electrical Systems and Information Technology, Volume 4, Issue 3, 2017, Pages 347-358, ISSN 2314-7172, https://doi.org/10.1016/j.jesit.2017.01.003.

[11] Zhang, Ningyun & Tang, Houjun & Yao, Chen. (2014). A Systematic Method for Designing a PR Controller and Active Damping of the LCL Filter for Single-Phase Grid-Connected PV Inverters. Energies. 7. 3934-3954. 10.3390/en7063934.

[12] A. Dell'Aquila, M. Liserre, V. G. Monopoli and P. Rotondo, Overview of PI-Based Solutions for the Control of DC Buses of a Single-Phase H-Bridge Multilevel Active Rectifier, in IEEE Transactions on Industry Applications, vol. 44, no. 3, pp. 857-866, May-june 2008.

[13] T. Esram and P. L. Chapman, Comparison of photovoltaic array maximum power point tracking techniques, IEEE Trans. Energy Convers., vol. 22, no. 2, pp. 439-449, Jun. 2007.

[14] Remus Teodorescu, Marco Liserre, Pedro Rodríguez Grid Converters for Photovoltaic and Wind Power Systems, 2011 John Wiley & Son, Ltd.